

New developments in Solar Neutrino Physics

Gianpaolo Bellini
Department of Physics
Universita' di Milano
Istituto Nazionale di Fisica Nucleare - Sezione di Milano
I-20133 Milano, ITALY

1 Introduction

In this paper I summarize the experimental results obtained in this last year on the solar neutrino physics; in addition the open problems in the Solar Standard Model are briefly discussed. The new experimental results concern SNO, third phase, Kamland and especially Borexino, which started to take data in may 2007, opening a window on the solar neutrino spectrum at very low energy.

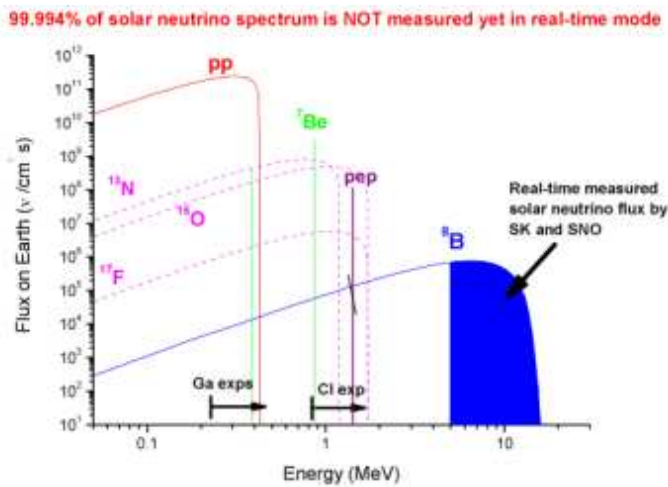


Figure 1:

Until now the experiments in real time (SNO and Superkamiokande) studied the solar neutrino flux only over a 4.5-5. MeV, exploring only about 1/10000 of the total solar spectrum (Figure 1). The reason of the choice of a so high threshold is the low rate of the neutrino events compared to the background produced by the natural

radioactivity, which is present everywhere, in the environment, in the construction and in the detecting materials. The threshold at 4.5-5. MeV is over the highest energy of radioactive decay of the two natural families, the Tl decay into $e^- + \gamma$.

The start up of the Borexino experiment, able to measure in real time the ν events with a threshold down to 200-250 keV, opens a new era in the study of the solar neutrinos.

I will try also to show that the study of the solar neutrinos is able to produce important insights both in the elementary particle physics and in the Sun physics.

2 Open problems in the Solar Standard Model.

The fluxes of the solar neutrinos are predicted by the Solar Standard model, which has been developed in the last 40 years, together with the density profile and the He abundances, These evaluations can be checked by means of the results of the neutrino experiments, of the solar Luminosity and by studying the helioseismology. The input data of the model are the Opacity (the photon mean free path in the Sun), the metal abundances and the cross sections of the various nuclear reactions taking place in the Sun. As an example the flux of the neutrinos from ${}^7\text{Be}$ depends from:

$$\Phi({}^7\text{Be}) \approx S_{33}^{-0.43} \cdot S_{34}^{-0.86} \cdot L^{+3.40} \cdot O^{-1.49} \cdot (Z/X)^{-0.62} \quad (1)$$

where S_{ij} are the cross section factors, L the solar luminosity, O the Opacity, (Z/X) the metal abundances. The solar neutrino experiments can improve the parameter errors of the Solar Standard Model by measuring the neutrino fluxes, corrected with the oscillation model, to determine Opacity, Diffusion, S-factors, Z/X ratio. But the S factors can be measured also directly in high precision experiments in Laboratory.

It is the case of Luna [1], which measured S_{34} and S_{33} for the reactions ${}^3\text{He} + {}^4\text{He} \rightarrow \alpha + 2p$ and ${}^3\text{He} + {}^3\text{He} \rightarrow {}^7\text{Be} + \gamma$, respectively. These two reactions belong to the pp chain: the first controls the ${}^7\text{Be}$ neutrino flux, while the second determines the pp chain branching ratio. S_{34} has been measured at 93 keV, allowing a good extrapolation to the Gamow peak: this precise value makes possible an important reduction of the uncertainty affecting the ${}^7\text{Be}$ and ${}^8\text{B}$ fluxes. S_{33} has been measured directly at the Gamow peak and its value confirmed the pp B.R., adopted until now by the Solar Model.

In addition LUNA obtained a good determination of $S_{1,14}$, which is connected to the reaction ${}^{14}\text{N}(p, \gamma){}^{15}\text{O}$, the slowest process in the CNO chain. This experimental determination reduces the CNO flux of $\approx 50\%$.

Recently S_{34} has been measured also by Brown et al. [2], but at higher energy (330 keV); their results are consistent with the LUNA data.

An important open problem in the SSM is the metallicity. The solar surface abundances of metals are determined from the analysis of the photospheric atomic and

Source	BPS _{high} Z	BPS _{low} Z	Difference
PP	5.97(1 ± 0.007)	6.04(1 ± 0.007)	0.07 ± 0.06
pep	1.41(1 ± 0.011)	1.45(1 ± 0.011)	0.04 ± 0.02
hep	7.90(1 ± 0.16)	8.22(1 ± 0.16)	0.30 ± 1.70
⁷ Be	5.08(1 ± 0.06)	4.55(1 ± 0.05)	0.53 ± 0.35
⁸ B	5.95(1 ^{+0.10} _{-0.09})	4.72(1 ^{+0.10} _{-0.09})	1.2 ± 0.8
¹³ N	2.93(1 ^{+0.15} _{-0.13})	1.93(1 ^{+0.15} _{-0.13})	1.0 ± 0.6
¹⁵ O	2.20(1 ^{+0.17} _{-0.14})	1.37(1 ^{+0.17} _{-0.14})	0.8 ± 0.4
¹⁷ F	5.82(1 ^{+0.17} _{-0.14})	3.25(1 ^{+0.17} _{-0.14})	2.6 ± 1.2

Table 1:

molecular spectral lines. Until the beginning of 2000, the associated solar atmospheric modeling has been done in one dimension, using a time-independent hydrostatic analysis, which incorporates the convection [3]. This treatment produces results in good agreement with the helioseismology observations.

More recently [4] a much improved three-dimensional treatment of the solar atmosphere reproduces better the profiles and brings the Solar abundances into a better agreement with other stars in the neighborhood. But the agreement with the helioseismology observations is much worse in comparison to the one-dimensional model. Following this improved analysis, the solar surface should contain 30-40% less carbon, nitrogen, oxygen, neon and argon, than previously believed.

The different values of the metallicity change the ν flux of solar reactions. In table 1 the neutrino fluxes expected with high and low metallicity are shown [5]. In the table the following units are used: $10^{10} \text{ cm}^{-2} \text{ s}^{-1}$ for pp, 10^9 for ⁷Be, 10^8 for pep, ¹³N, ¹⁵O, 10^6 for ⁸B and ¹⁷F, 10^3 for hep.

In some cases the differences between high and low metallicity are larger than the model errors; in the case of ⁷Be and ⁸B they are borderline, while for the CNO cycle the difference is $\sim 50\%$. Then precise experimental measurements of solar neutrino fluxes can help in fixing the Z/X problem.

3 Recent results on solar neutrinos over 5 MeV.

SNO and Kamland have recently released new results. The SNO new data concern the so-called phase 3. As it is well known SNO is a Cherenkov experiment using heavy water; three different neutrino interactions are detected: Charged currents, CC ($\nu_e + d \rightarrow p + p + e^-$), Neutral currents, NC ($\nu_x + d \rightarrow n + p + \nu_x$), elastic scattering on electron, ES. The neutral current interactions are tagged by the neutron capture with the emission of γ s; the neutron is captured by the deuterium in the first phase (just $D_2O : n + d \rightarrow t + \gamma + 6.25 \text{ MeV}$), by the ³⁵Cl in the second phase ($D_2O + 2$

tons of NaCl: $n + {}^{35}\text{Cl} \rightarrow {}^{36}\text{Cl} + \gamma + 8.6\text{MeV}$), by ${}^3\text{He}$ in the third phase ($36\text{ }{}^3\text{He}$ proportional counters inserted in the detector: $n + {}^3\text{He} \rightarrow p + t + 0.76\text{MeV}$).

The data of the third phase are collected in 387.17 live days [6]. The detection efficiencies are determined by a neutron calibration source (${}^{252}\text{Cf}$, ${}^{241}\text{AmBe}$) and via γ s produced by activated NaCl.

The rates of the three reactions are compared with the first and second phase in Figure 2 (from left to right: CC, NC, ES). The agreement is in general good but for the elastic scattering where the results differ $\sim 1.5\sigma$. The ratio between the CC and NC reactions is in good agreement with the ones obtained in the first two phases ($\frac{\Phi_{CC}}{\Phi_{NC}} = 0.301 \pm 0.033$).

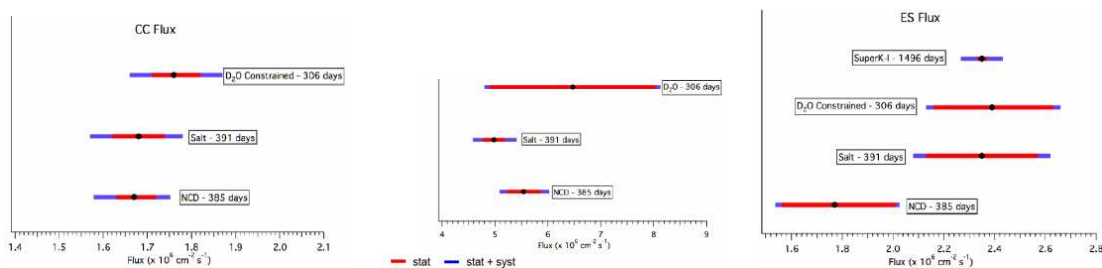


Figure 2:

As it is known, Kamland is a scintillator experiment which studies the antineutrinos produced by the Japanese reactors, with an average distance of 180 km and average energy of ≈ 1.8 MeV. The reaction detected is $\bar{\nu} + p \rightarrow e^+ + n$, with a prompt signal due to the e^+ annihilation, and a delayed one (about $200\mu\text{s}$) due to the neutron capture from ${}^{12}\text{C}$ or H nuclei. In 1490.8 ± 0.5 days of data taking they observe 1609 $\bar{\nu}$ interactions, to be compared with the expected number with no oscillation of 2179 ± 89 . The background is estimated to be 276.1 ± 23.5 [7].

In Figure 3 the energy spectrum of the detected interactions is compared with the expected one in the hypothesis of no oscillation, and with the background. In Figure 4 two oscillation periods are shown plotting the $\bar{\nu}_e$ survival probability vs $L_0/E_{\bar{\nu}_e}$, profiting of the relatively wide energy spectrum of the reactors antineutrinos.

The best fit values of the oscillation parameters, Δm^2 , $\tan^2\theta$, obtained from the results of Kamland released in 2008, from the SNO all data collected in the three phases, from all solar experiments data collected until 2005 plus the Kamland data, from solar experiments including 2008 results + Kamland, are quoted in Figure 5.

In general there is a certain agreement among the various best fit values, except for SNO total, which is quoted without errors. As it is shown in Figure 6 (a), when the total SNO data are fitted, the allowed regions include oscillation parameters that are outside the LMA region, and the Δm^2 parameter has two minima that are widely separated: this creates a problem in obtaining reasonable errors.

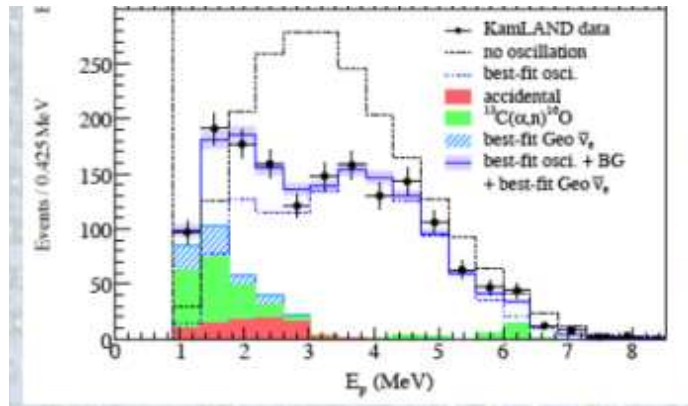


Figure 3:

The allowed regions are shown in Figure 6(b), for all data produced by the solar experiments (Cl, Ga, Superkamiokande, SNO, Borexino) and in Figure 6(c) for all solar plus Kamland. There is a disagreement in the best fit value for Δm^2 ; the difference between solar only and solar plus Kamland is due more probably to θ_{13} , which could be not zero [8].

In Figure 7 the survival probability of ν_e as a function of the neutrino energy is shown. The continuous line reproduces the oscillation model calculated for ^8B neutrinos by using, for the oscillation parameters, the best fit values quoted in the last line of Figure 5. The points refer to the data obtained by the real time solar neutrino experiments before the Borexino start up (high metallicity has been assumed), and the constraints that all the experiments on solar neutrinos produced on pp and ^7Be fluxes.

4 Borexino.

4.1 The detector

Borexino is the first and only experiment, until now, able to study in real time the solar neutrino flux at or below 1 MeV of energy. It is installed in the Gran Sasso underground laboratory.

The Borexino design and layout are shown in Figure 8. The design is based on the principle of graded shielding and increasing radiopurity going from the external to the more internal shells. The detecting material of 300 tons is a binary scintillator (Pseudocumene [Pc] plus PPO), surrounded by a liquid buffer, consisting of Pseudocumene added with a quencher (DMP) [9].

The main feature of the Borexino detector is the very low radiopurity, never

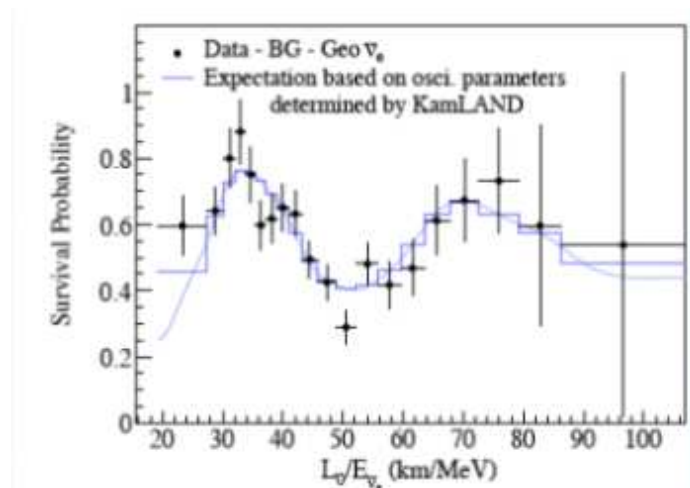


Figure 4:

achieved until now in experiments at ton level. To reach this goal, many special methods and tools have been developed, along five years of R&D. The main items concern: a) the scintillator cleaning by means of: water extraction, low temperature distillation (80 mbar, 90-95 °C), nitrogen stripping, ultrafine filtration; b) use of ultrapure N₂, at record levels, for stripping: Rn free Nitrogen (Rn < 0.1 μBq/m³), LAK Nitrogen (Ar content: 0.01 ppm, Kr: 0.03 ppt); c) special care in the Pc procurement: old layers crude oil (to minimize the ¹⁴C), special loading station (maintained in N₂ atmosphere) directly connected to the production plant, special shipping vessels, rapid transport to the underground laboratory (to minimize the cosmogenic production of radioactive nuclides, as ⁷Be); d) extreme precaution in the fabrication and assembly of the Nylon Vessels: selection and extrusion of the material in controlled area, construction in clean room with Rn control, special bag for shipping; e) all surface electropolished of: detector components, lines, fittings, valves; f) special developments and selection of the components (as for the PMTs); g) any operation in clean room or in N₂, Ar atmosphere.

In addition, in order to check the ultra-low radioactive levels, a very high sensitivity detector (down to $5 \cdot 10^{-16}$ g/g U, Th equivalent, $\approx 10^{-18}$ ¹⁴C/¹²C) has been installed underground, the Counting Test Facility (C.T.F.).

The background measured in Borexino during about 200 days of data taking is the following: ¹⁴C/¹²C: $(2.7 \pm 0.6) \cdot 10^{-18}$; ²³²Th equivalent: $(6.8 \pm 1.5) \cdot 10^{-18}$ g/g from the coincidence ²¹²Bi-²¹²Po; ²³⁸U equivalent: $(1.6 \pm 0.1) \cdot 10^{-17}$ g/g from the coincidences ²¹⁴Bi-²¹⁴Po. In addition two contaminants have been found in the detector: ⁸⁵Kr, despite the very high purity N₂ used for the stripping, and ²¹⁰Po without any evidence of ²¹⁰Bi.

	$\Delta m^2 (eV)^2 \cdot 10^{-5}$	$\tan^2 \theta$
Kamland 08	$7.58^{+0.14}_{-0.13} \pm 0.15$	$0.56^{+0.10+0.10}_{-0.07-0.06}$
SNO total 08	4.57	0.447
Solar 05 + Kamland	7.59 ± 0.21	$0.47^{+0.06}_{-0.05}$
Cl-Ar, SK, Sage, Gallex SNO 08, Borex Kamland.	$7.94^{+0.42}_{-0.26}$	$0.448^{+0.05}_{-0.04}$

Figure 5:

The Kr is measured via the coincidences of the two following decays: $^{85}Kr \rightarrow ^{85m}Rb \rightarrow ^{85}Rb$, with the emission of a 173 keV β , followed by a 514 keV γ , with $\tau = 1.46 \mu s$. Unfortunately this decay has a B.R. of only 0.43%: 8 events have been measured in the data taking period, corresponding to 29 ± 14 c/d.

The nuclide ^{210}Po is present despite the precision cleaning of the lines; this nuclide is very mobile and easily sticks on the internal surface of the pipes, and it is released little by little. At the beginning its rate was ~ 80 c/d/ton; now it is reduced to ~ 10 c/d/ton with a decay time very close to the nominal one (200 d).

4.2 The Borexino science goal.

The main reaction studied in Borexino is the $\nu - e$ elastic scattering.

The first observation of sub-Mev neutrinos in real time is the first design goal of Borexino, with the aim of testing the MSW effect with the LMA solution at very low energy, and then the existence of two regimes of oscillation: in vacuum and in matter. A good determination of the 7Be flux, at or below 5%, would provide also a strong constraint on the pp flux, allowing a check of the balance between photon and neutrino luminosities in the Sun. Another item included in the original project is the measurement of the 7% seasonal variation of the neutrino signal, following the Earth's orbital eccentricity.

But the radio-purity measured with the first Borexino data is much better than the design prescriptions; this extraordinary achievement opens further possibilities,

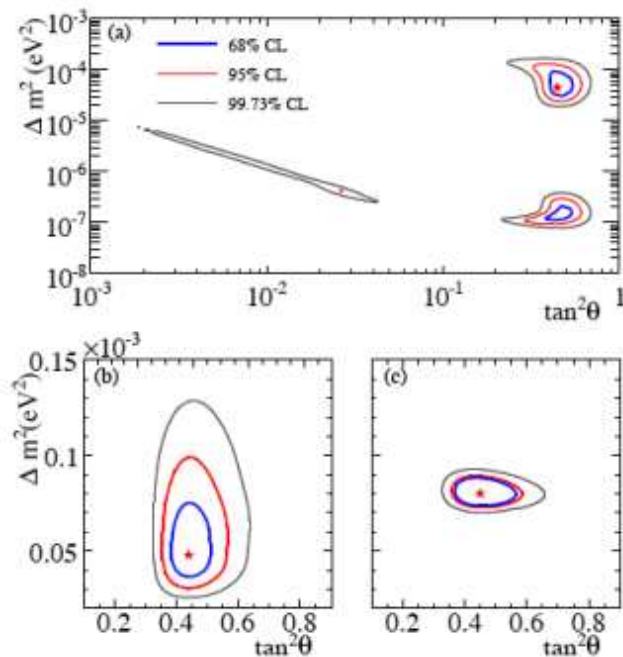


Figure 6:

as the experimental determination of the pep neutrino flux, possibly the pp flux, and the neutrinos from ${}^8\text{B}$ with a threshold down to 2.8 MeV.

Other items of the Borexino scientific program are: the study of the $\bar{\nu}_e$ emitted by the Earth; the detection of a Supernova explosion, if any; a competitive upper limit for the neutrino magnetic moment.

4.3 Measurement of the ${}^7\text{Be}$ neutrino flux and check of the existence of a vacuum regime in the oscillation model.

In Figure 9 all data are shown (black line), once vetoed or subtracted the muons, the events muon induced (within 2 ms after the muon) and the ${}^{222}\text{Rn}$ daughters. In the same figure the blue line shows the data after the fiducial cut, and the red line, after αs subtraction via the α/β discrimination. The blue bump, shown before the αs subtraction, is due to the ${}^{210}\text{Po}$ (which has a $Q=5.41$ MeV, quenched in the Borexino scintillator with a factor ≈ 13).

The α/β is carried out by means of the Gatti parameter [10] [11], based upon references curves obtained in Borexino from the analysis of the ${}^{222}\text{Rn}$ decay, during the filling operations.

In Figure 10 (left) the neutrino event distribution, once subtracted the αs , is fitted

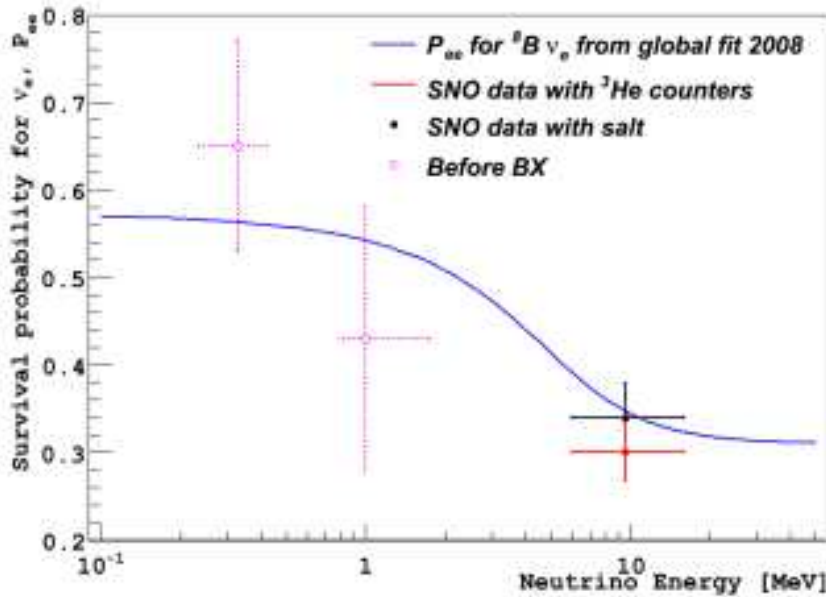


Figure 7:

living ${}^7\text{Be}$, ${}^{14}\text{C}$, $\text{CNO}+{}^{210}\text{Bi}$, ${}^{11}\text{C}$, ${}^{83}\text{Kr}$ and the light yield as free parameters, while the pp and pep fluxes are fixed at the values predicted by the Solar Standard Model. The CNO and the possible ${}^{210}\text{Bi}$ are fitted together because their spectra are very similar. The ${}^{11}\text{C}$ is produced by the residual muons in the underground Gran Sasso Laboratory (see later).

It has been preferred to leave as free parameters the ${}^{83}\text{Kr}$ and the light yield, even if they are measured directly. The first is determined, as already explained, via the decay coincidence ${}^{85}\text{Kr} \rightarrow {}^{85\text{m}}\text{Rb} \rightarrow {}^{85}\text{Rb}$, but, due to its very small B.R., the statistics is still not enough for a precise measurement; the second is fitted directly by exploiting the well known spectrum of ${}^{14}\text{C}$, ${}^{210}\text{Po}$ and the position of the ${}^7\text{Be}$ shoulder, due to the Compton edge. The fit results for both are fully consistent with the direct measurements.

In Figure 10 (right) a similar fit is carried out on the neutrino spectrum, but without α subtractions: a threshold is imposed at 250 keV of energy, while the free parameters are the same as in the previous fit, with the difference that now the ${}^{210}\text{Po}$ is added.

The results of the two fits are fully consistent each other. In particular for the ${}^7\text{Be}$ flux the rate in both cases is: 49 ± 3 cpd/100 tons [12]. Here the quoted error is statistical only.

The systematic errors concern the definition of the Inner Vessel position and the

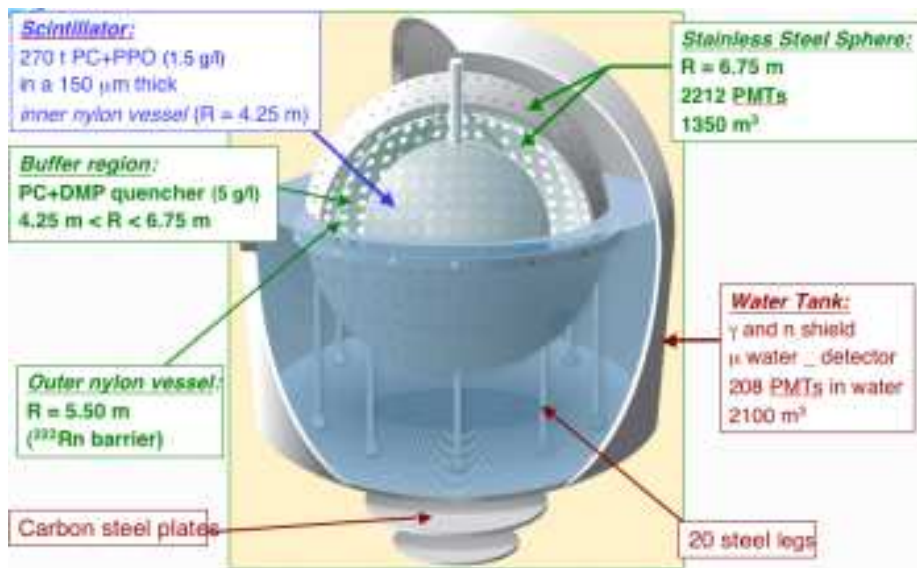


Figure 8:

detector response function. Both are determined until now exploiting internal signals and the ones emitted by the Inner vessel walls; the precision in fixing these two parameters will be much improved with a calibration campaign, already scheduled, by means of external sources.

Finally the 862 keV ${}^7\text{Be}$ solar ν rate in Borexino is: $49 \pm 3_{stat} \pm 4_{syst}$ cpd/100 tons, corresponding to a flux: $\Phi({}^7\text{Be}) = (5.12 \pm 0.51) \cdot 10^9 \text{cm}^{-2}\text{s}^{-1}$, which has to be compared to the high metallicity prevision of $(5.8 \pm 0.56) \cdot 10^9 \text{cm}^{-2}\text{s}^{-1}$ and to the low metallicity one, $(4.55 \pm 0.5) \cdot 10^9 \text{cm}^{-2}\text{s}^{-1}$. The quoted errors do not allow, for the moment, to discriminate between the two SSM expectations. The goal of Borexino is to reach a total error for the ${}^7\text{Be}$ flux below 5%.

In Figure 11 the ν_e survival probability as function of the neutrino energy is plotted. The MSW previsions (continuous and dashed lines) are calculated following the LMA solution with $\Delta m_{12}^2 = 7.94 \cdot 10^{-5} \text{eV}^2$ and $\tan^2\theta = 0.447$, as obtained from the global fit on the data up-to-dated to 2008. The points for ${}^7\text{Be}$ are the Borexino results, calculated for both the SSM hypotheses of high and low metallicity, while the ones for pp correspond to the pp flux constrained by the Borexino data.

The pp and CNO fluxes, as constrained by the Borexino data, are shown also in Figure 12.

The ${}^7\text{Be}$ ν spectral shape vs the recoiled electron energy has been studied to find possible e.m. components due to the ν magnetic moment: the limit of 5.4 Bohr magneton has been found, which is the lowest limit obtained until now.

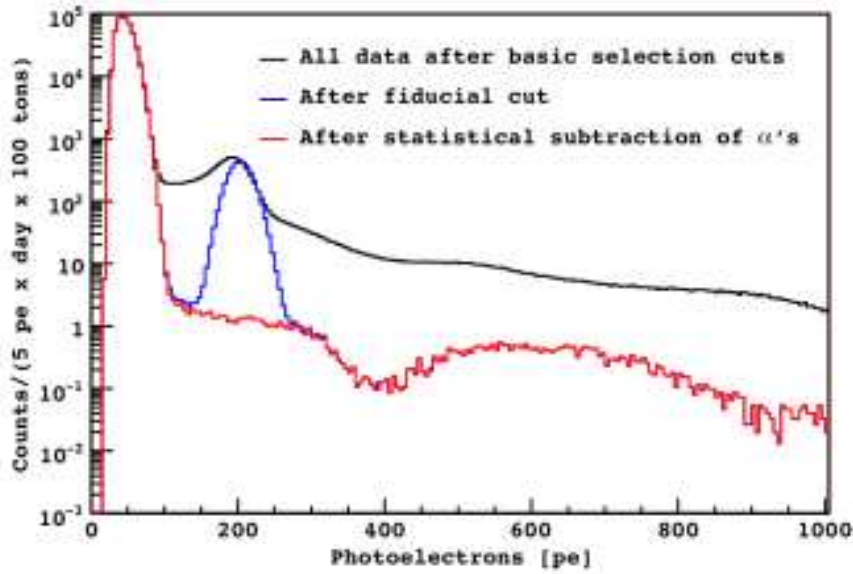


Figure 9:

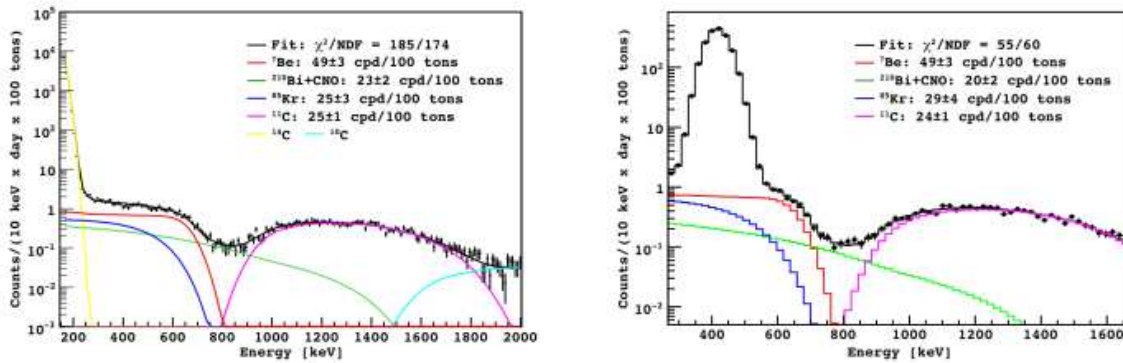


Figure 10:

4.4 What next.

The next goals of Borexino are: the ^7Be measurement with a total error at or below 5%, and possibly the direct determination of the pp flux. This last measurement could be obtained analyzing the energy window 190-230 keV, where the background is under control.

The pep flux is a further goal. To achieve it, much more statistics is needed (2 cpd/100 tons are expected in Borexino, following the SSM prevision), and a good

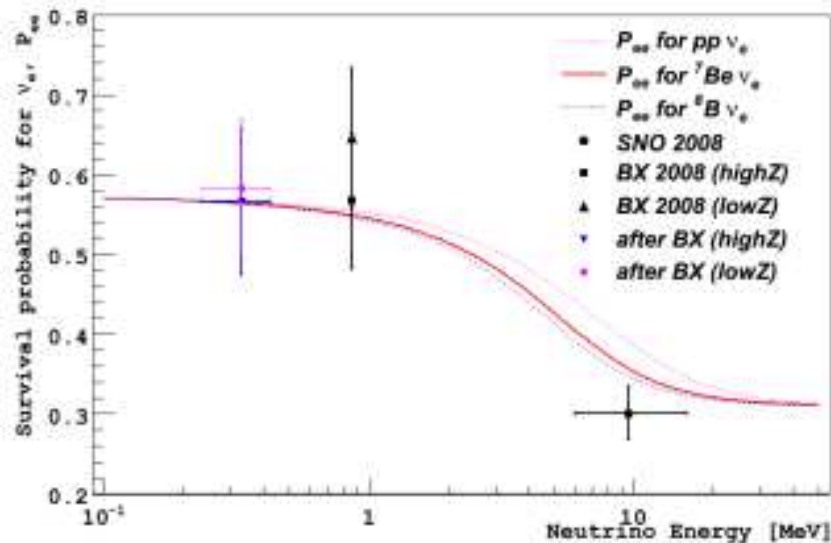


Figure 11:

identification of the ^{11}C nuclides, produced by the cosmic muons in the Gran Sasso underground laboratory ($1.1 \mu \text{ m}^{-2}\text{h}^{-1}$ with $\langle E_\mu \rangle = 325 \text{ GeV}$) is necessary. The cosmogenic ^{11}C are identified via a threefold coincidence among: the muon (which produces the $^{11}\text{C} : \mu + ^{12}\text{C} = ^{11}\text{C} + n + \mu$), the ^{11}C decay ($^{11}\text{C} \rightarrow ^{11}\text{B} + e^+ + \nu_e$), and the n capture (with the emission of a 2.2 MeV γ). This method has been tested successfully in C.T.F. [13]. The read out electronics has been implemented in Borexino to detect all the neutrons produced by each incident muon, which in some cases reach the number of 100. A rejection percentage of about 90% has been already achieved, but the work is still in progress.

Another study in progress is the detection of antineutrinos from the Earth, which is made easier in Gran Sasso due to the very low background of antineutrinos emitted by nuclear reactors on that site.

5 Conclusions.

There are still open problems in the Standard Solar Model, as it is the case for the metallicity, and many parameters are still unknown. Some important S factors have been measured in laboratory; precise experimental determinations of the neutrino fluxes can provide important insights in the Model.

Until now the scheme MSW-LMA has not been denied at low energy by the Borexino data on the ^7Be flux, but more efforts and statistics are needed to give a

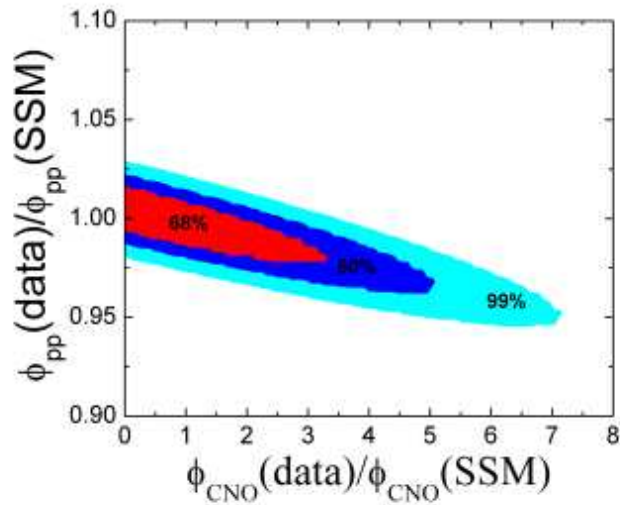


Figure 12:

final check of the oscillation model. In the meantime the vacuum oscillation regime has been found experimentally by Borexino.

Due to the very high radiopurity, Borexino seems able to measure other low energy solar neutrino fluxes, as pep and probably pp; the Borexino data produced already a strong constraint on the pp flux. But these measurements need a lot of care: Borexino estimates other two years to reach the final results.

References

- [1] C. Brogini, talk at this Conference.
- [2] T.A.D. Brown et al., Phys. Rev. **C76**, 055801 (2007).
- [3] N. Grevesse et al., Space Sci. Rev. **85**, 161 (1998).
- [4] C. Allende Prieto et al., Astrophys. J. **573** L137 (2002); C. Allende et al., Astrophys. J. **556**, L63 (2001).
- [5] C. Pena-Garay and A.M. Serenelli, private communication.
- [6] SNO collaboration; B. Aharmin et al., arXiv: 0806.0989v1, June 2008.

- [7] J. Shirai, New Kamland results, Neutrino Oscillations in Venice, Proceedings Istituto Veneto di Scienze, Lettere ed Arti, pag. 447.
- [8] G.L. Fogli et al., Phys. Rev. Lett. **101**, 141861 (2008).
- [9] Borexino Collaboration, G. Alimonti et al., arXiv: 0806.2400, oct. 2008, to be published at N.I.M.
- [10] E. Gatti et al., Nuclear Electronics, **2** IAEA, Wein 265 (1962).
- [11] Borexino Collaboration, E. Back et al., Nucl. Instr. and Methods **A584**, 98 (2008).
- [12] Borexino Collaboration, C. Arpesella et al., PRLB **101**, 091302 (2008).
- [13] Borexino Collaboration, Phys. Rev. **C74**, 045805 (2006).